

2.1 Hazard

In the modelling approach, hazard is represented by inundation maps showing flood extent and depth for different return periods (1, 2, 5, 10, 25, 50 and 100 years). These hazard maps are developed using the SOBEK Hydrology Suite, which
5 employs a Sacramento rainfall/runoff and a 1-D/2-D hydraulics model (Deltares, 2014). For current conditions, the input data and hydraulics schematisation use 2012 measurements gathered by the Flood Hazard Mapping (FHM) project and the Flood Management Information System (FMIS) project (Deltares et al., 2012), and precipitation data from the National Bureau for Meteorology (BMKG).

10 In this study, we also simulated inundation maps (for each return period) for different future scenarios of climate change and land subsidence. To simulate impacts from climate change, we forced the model with changes in two factors: sea-level rise and precipitation intensity.

Changes in precipitation intensity were simulated using bias-corrected daily data on precipitation for 5 General Circulation Models (GCMs), obtained from the ISI-MIP project (Inter-Sectoral Impact Model Intercomparison Project) (Hempel et al., 2013). These data are available at a horizontal resolution of $0.5^\circ \times 0.5^\circ$, and have been bias
15 corrected against the EU-WATCH baseline reanalysis dataset (Weedon et al., 2011) for the period 1960–1999. Future climate data were used for five GCMs, namely: GFDL-ESM2M, HadGEM2-ES, IPSL-CM5A-LR, MIROC-ESM-CHEM, and NorESM1-M, and for the following Representative Concentration Pathway (RCP) scenarios: RCP2.6, RCP4.5, RCP6.0, and RCP8.5. Thus, we used 20 GCM-RCP combinations in total. We calculated change factors in daily precipitation volume between the baseline climate
20 dataset and each GCM-RCP combination, for each of the return periods used in this study. The extrapolation to the different return periods is carried out by fitting the Gumbel distribution to the time-series of annual maximum precipitation, whereby the Langbein correction (Langbein, 1949) is applied for return periods lower than 10 years. We carried out this statistical process for each of the GCM-RCP combinations for two
25

4439

time-periods, namely 2010–2049 and 2040–2079. These time-periods are used in the paper to represent climate conditions in 2030 and 2050, respectively. Finally, these change factors were applied to the standard input of the SOBEK model under current conditions, which is based on gauged precipitation data at 29 stations.

5 In the SOBEK model, sea-level is used as a boundary condition at the river–sea interface. Therefore, we used two simple scenarios of sea-level rise between 2010–2030 and 2010–2050, and added these to the SOBEK input baseline sea-level for 2010. These low and high scenarios represent the 5th and 95th percentiles of the global sea level rise projections of the IPCCs Fourth Assessment Report (AR4) (IPCC,
10 2007), using the method of Meehl et al. (2007). The scenarios represent increases in sea-level of 3 and 11 cm respectively for the period 2010–2030; and 6 and 21 cm respectively for the period 2010–2050.

Finally, we also produced hazard maps showing the magnitude of continued land subsidence. This was done by subtracting projections of future subsidence from the
15 Digital Elevation Model (DEM) used in SOBEK (Deltares et al., 2012; Tollenaar et al., 2013). The DEM has a horizontal resolution of $50\text{ m} \times 50\text{ m}$. In SOBEK, the original DEM is replaced by the new DEM (with future subsidence), and the hydrological-hydraulic simulations are repeated. This results in new flood hazard maps showing the flood inundation and extent under the land subsidence scenario, which are then used as
20 input to the Damagescanner-Jakarta model. A map showing the spatial distribution of the projected land subsidence between 2012 and 2025 used in our model setup is shown in Fig. 2. We used a hypothetical scenario of land subsidence, in which the current rate of subsidence (Abidin et al., 2011) continues at the same rate, and ultimately stops in the year 2025. The latter is due to the large uncertainty of predicting
25 the displacement and rebuilding of weirs, dikes, and bridges in the hydraulic model input, rather than a theoretical ultimate level of land subsidence. The current rate of subsidence ranges from $1\text{--}15\text{ cm year}^{-1}$ across different parts of the city (see Fig. 2). This simple approach is used in the absence of more detailed scenarios of future land

4440

3 Results

This section is split into three subsections. Firstly, we describe the flood risk results under current conditions in comparison to past results reported in Budiyo et al. (2014) to show the change resulting from the new model schematisation and the newly operational flood protection measures. Secondly, we show the potential impacts of climate change on extreme precipitation, one of the drivers of risk change discussed in this paper. Thirdly, we show the potential changes in flood risk between the current situation and the future, based on the various future scenarios. We examine both the individual and combined influence of the different drivers on flood risk.

3.1 Flood risk under current conditions

In this study, we ran Damagescanner as described in Sect. 2. The resulting flood risk under current conditions is USD 143 million p.a. This is significantly lower than our past result as presented in Budiyo et al. (2014), in which flood risk was estimated to be USD 321 million p.a. The differences are due to changes that have been carried out in the hydraulic system in Jakarta, which have been included in a revised schematisation of the hydrology model. The main changes are now discussed, and it appears that flood protection actions taken since 2007 have led to reduced flood hazard, and consequently flood risk, as reflected in the lower current risk estimate in this study.

The version of the hazard model used in Budiyo et al. (2014) used a hydraulic schematisation based on the situation in 2007. In the current paper, we used an updated version of the model in which the schematisation has been updated to include flood protection measures, including flood gates and weirs that have been implemented between 2007 and 2013. Moreover, the revised version of the model has a more accurate representation of those flood protection measures that were already in place in 2007. The most important single change in the hydrological and hydraulic situation that has taken place since 2007, and is now implemented in SOBEK, is the newly built Eastern Flood Canal (Banjir Kanal Timur, BKT), which diverts flood waters away from

4443

the eastern side of the city via the canal. Comparing the flood hazard maps for a given return period based on the 2007 and 2013 schematisations shows that the simulated flood extent in the eastern half of the city has indeed decreased. For example, in Fig. 4 we show the differences in inundation depth between 2007 and 2013; in the eastern half of the city, the flood extent has decreased by 27 % by width or by 34 % by volume.

The reliability of the new 2013 flood maps has been compared with empirical flood maps produced by the National Disaster Management Office (BNPB). These maps show which village administration (Kelurahan) units in Jakarta actually suffered from inundation during the 2007 and 2013 flood events (Fig. 5). We can see that the spatial pattern in the western half remains fairly similar, whilst far fewer Kelurahan were reported as suffering from inundation during the 2013 flood in the eastern part. It should be noted that the return periods of the floods in 2007 and 2013 are not exactly the same; the former is estimated to have a return period of ca. 50 years, compared to 30 years in the latter. Hence, the figure is only intended to demonstrate the fact that there appears to be an overall agreement between the 2013 modelling results and the Government flooding maps showing smaller inundation areas in the eastern parts as compared to previous research. This explains our lower risk estimates compared to Budiyo et al. (2014).

Finally the changes in the inundation depths are also partly due to further modifications of the SOBEK schematisation in terms of its hydraulics. Namely, the Saint-Venant equations have been implemented on more detailed dimensions of stream fractions, which produces finer 1-D overtopping and a more disperse but shallower 2-D floodplain.

3.2 Potential impacts of climate change on extreme precipitation

As described in Sect. 2.1, we estimated changes in the magnitude of 1 day precipitation sums for the different return periods used in this study, based on data from 5 GCMs and 4 RCPs, i.e. 20 GCM-RCP combinations. In Fig. 6, we present precipitation factors that show changes in extreme 1 day precipitation for different return periods, whereby

4444

and assuming no other changes in physical or socioeconomic factors, flood risk would increase between the current situation and 2030 by a factor of 1.1. More detailed results are presented in Table 5, which shows the percentage of both the total inundated area and damage (here shown from the map of a 5-year return period, which is the return period for which the damage is closest to the annual expected damage) associated with each land use class. Similar distributions of damage between the different land use classes are also found for the other return periods. The results show that the majority of the inundated areas are found in locations with residential land use classes. This is both the case under current land use (60%; summation of “high density urban kampung”, “low density urban kampung”, and “planned house”) and under 2030 land use (60%; summation of “residential” and “residential with greenery”). However, the largest share of total damages are found in the land use classes related to commercial areas, i.e. “Industry and warehouse” followed by “Commercial and business”. Combined, these two land use classes account for ca. 72% of total damages under current land use, and 77% under future land use.

3.3.3 Land subsidence

Assuming only an increase in land subsidence for 2030, we found an increase in annual expected damage of 173% between the current situation and 2030, i.e. an increase from USD 143 million p.a. to USD 391 million p.a.

The increase in risk resulting from projected subsidence, however, is not uniform across the city. In Fig. 7, we see the percentage increase in flood damage per grid cell over the period 2010–2030 due to subsidence alone, following the rates of subsidence shown in Fig. 2. Note also that the actual influence of subsidence will strongly depend on the changes in other environmental and socioeconomic drivers (as discussed in Sect. 4.3).

4447

3.4 Impacts of future changes in combined risk drivers on flood risk

In the previous subsections, the change in risk between the current situation and the future scenarios has been shown for each risk driver separately. In reality, the future situation will depend on the combined change of all the drivers. Hence, in this section we show the impacts of combinations of different risk drivers on future risk.

In Fig. 8, we show probability density functions (PDFs) of the simulated annual expected damage, whereby each PDF is derived from a 2-parameter Gamma distribution fit to the 20 GCM/RCP combinations. A similar approach was followed by Ward et al. (2014b) for including climate change in probabilistic projections of flood risk along the Rhine in Europe. The dotted black vertical line represents current flood risk, i.e. USD 143 million p.a.

Figure 8 clearly shows the strong influence of projected subsidence on the overall change in risk. All of the PDFs representing scenarios with subsidence (shown in red) show much higher annual expected damage than those without subsidence (shown in blue). The PDFs also clearly show the large uncertainty associated with the projected changes in precipitation from the different GCMs and RCPs, which is large under all of the PDFs. However, the results show that if we include land subsidence in the future projections, the probability of future flood risk exceeding current day flood risk exceeds 99.999% (when accounting for changes in precipitation).

The results also show the importance of the interaction between different drivers. For example, if we examine the difference between the PDFs for low and high sea level rise, we see a small difference under the scenarios with no subsidence and land use 2030. In this case, the median risk value (across the PDF of different GCM/RCP combinations) is 22% greater under the high sea level rise scenario (USD 174 million p.a.), while under the low sea level rise scenario decrease to be USD 138 million p.a. However, if we make a similar comparison using the scenarios that include subsidence, the median risk value is 34% greater under the high sea level rise scenario (USD 519 million p.a.) than under the low sea level rise scenario (USD 388 million p.a.). Similar

4448

differences can be found when comparing the scenarios with and without projected land use change. The differences between the two scenarios are amplified with higher rates of subsidence and/or sea level rise.

From Table 6, we summarize the results of the influence on risk of the individual drivers and the combined scenarios for 2030. For scenarios with climate change, we show both the median and 5th–95th percentile values based on the Gamma distributions. From the Table, it is clear that land subsidence has the largest influence on future risk, followed by land use change and sea level rise.

4 Discussion

4.1 Uncertainty in projections of change in precipitation intensity

In Sect. 3, we showed the impacts of climate change on flood risk, whereby the impacts of climate change are expressed through both sea level rise and changes in the magnitude of extreme 1 day precipitation totals. In terms of the latter, our analyses show this variable to be highly uncertain. Whilst the median projections (Table 3) show a decrease compared to baseline – which results in lower median flood risk in the future when combined with the low sea level rise scenario (Table 4) – the PDFs in Fig. 8 show that there is deep uncertainty attached to the impacts of changes in precipitation on the risk. Nevertheless, this does not mean that it is not an important factor to consider. In fact, some of the GCM-RCP combinations indicate an increase in risk of a factor greater than 2.7 as a result of climate change alone.

The uncertainty in future risk projections is confirmed by other research in the region. For example, rainfall observations across Indonesia as a whole for the second half of the 20th century suggest that mean annual rainfall may have decreased by ca. 2–3%, mainly in the wet season from December to February (Boer and Faqih, 2004). Earlier projections of mean annual rainfall over the 21st century taken from several climate models suggest that mean annual rainfall may increase in the future across

4449

most of Indonesia, although in Java it may decrease (Hulme and Sheard, 1999). Naylor et al. (2007) downscaled output from the Intergovernmental Panel on Climate Change AR4 suite of climate models for the 21st century, to the regional level, and found a large uncertainty on the monsoon onset in West Java/Central Java region. Moreover, they found that precipitation totals may decrease (by up to 75% in the tails) during the dry season, although this research did not address the wet season, when flooding generally occurs in Jakarta. Scoccimarro et al. (2013) investigated potential changes in extreme precipitation events by 2100 using RCP8.5 and several CMIP5 models. They found that the 90th and 99th percentiles of heavy rainfall may increase during the months June–August in Indonesia. However, this is the dry season, whilst flooding in Jakarta usually occurs during the wet months of December–February.

Recently, Chadwick et al. (2013) carried out climate model experiments to assess the potential changes in regional patterns of precipitation and atmospheric circulation resulting from a “ramp-up” of CO₂ levels from pre-industrial levels (280 ppm) until quadrupling (1120 ppm) after 70 years (and scenarios of 3 × CO₂, 2 × CO₂, and 1.5 × CO₂), followed by 10 years of stabilisation, and then a 70-year ramp-down to pre-industrial levels. During the ramp-up phase, they found decreased precipitation in the part of the tropical western Pacific where Indonesia is located. Chadwick et al. (2013) suggest that this regional redistribution of rainfall is caused by circulation changes associated with changing gradients of sea-surface temperatures (SSTs) in the tropical Pacific.

Further uncertainties in the future response of precipitation to climate change in the region result from potential changes in the frequency and/or magnitude of El Niño Southern Oscillation (ENSO). ENSO shows strong linkages with precipitation in parts of the Indonesian archipelago (Aldrian and Susanto, 2003; Aldrian et al., 2007; Hendon, 2003; Qian et al., 2010), and is linked to anomalies in both discharge (Poerbandono et al., 2014) and flood volumes (Ward et al., 2014a). The current generation of climate models shows little agreement on whether (and if so how) the frequency of ENSO could change due to climate change (Guilyardi et al., 2009; Paeth et al., 2008; Van

4450

Jakarta is (Abidin et al., 2011). Soil water extraction takes place both for supplying water for drinking and industry, as well as in the construction of high-rise buildings. PDAM Provinsi DKI Jakarta (2012), the water industry board of Jakarta, supplies water to 61.1% of consumers in Jakarta. They report that an additional $8\text{--}10\text{ m}^3\text{ s}^{-1}$ would be needed to erase the need for all deep wells while sufficing the needs of the rest presently not sufficed. According to a synthesis of results in reports by PAM Lyonaise Jaya (2012) and Aetra Air Jakarta (2013) this would require an investment of ca. USD 389 million. Whilst this is a large investment, it is of the same order of magnitude as our projected increase in risk per annum resulting from land subsidence, land use change, and climate change. Hence, whilst this is a very simplistic example, it shows that measures to increase and improve water supply appear to be small in relation to the damages that they could help to avoid, even without factoring in the other benefits. Indeed, strict regulations on groundwater pumping (accompanied by the supply of alternative water sources) have been shown to be effective in reducing land subsidence. For example, the rate of subsidence in Bangkok was ca. 12 cm year^{-1} during the 1980s, but was reduced to 2 cm year^{-1} after strict regulations on deep well pumping (Phien-wej et al., 2006). A nested modelling approach by Aichi (2008) has shown that the groundwater regulations in Tokyo have led to decreased subsidence since the mid-1970s. The groundwater regulation was effective for Tokyo and the surrounding three prefectures for 14 years from January 1961 until April 1974 (Tokunaga, 2008). As mentioned earlier, high-rise building construction also extracts water from the soil (dewatering) during the process. This intensive extraction of soil water in the short term has been reported to result in severe localised land subsidence (Zhang et al., 2013). Hence, it may also be useful to consider other piling processes, such as auger piling (Abdrabbo and Gaaver, 2012). If dewatering is unavoidable for Jakarta, it may be useful to focus such high-rise development in those parts of the city where the lithology is more compacted, such as in the southern part (Bakr, 2015).

In this study, we represent changes in land use by using a single scenario, which refers to an idealised plan of the city in 2030, assuming that the land use planning

4453

for 2030 is implemented. Our results show that under this scenario (land use change alone), risk would increase by 15%. Given the fact that changes in exposure through urban development are seen as one of the main drivers of risk in developing countries (Jongman et al., 2012; UNISDR, 2013), such a relatively low increase in risk attributable to land use change would be encouraging. Moreover, the scenario does not include assumptions on potential measures or strategies that could be taken to further reduce flood risk. For example, in Indonesia as a whole, Muis et al. (2015) simulated increases in both river and coastal flood risk by 2030 assuming a scenario where building is allowed in flood-prone areas, and several scenarios where new buildings are prohibited (with different levels of enforcement) in the 100-year flood zone. They found that river flood risk could be reduced by about 30–60%, and coastal flood risk by about 65–80%, compared to the scenario in 2030 with no building restrictions in the flood-prone zone. Also, measures could also be taken that allow for building in flood-prone areas, but only if certain building codes are used. For example, dry-proofing and wet-proofing of houses have been found to have a large potential to decrease flood risk (e.g. Kreibich et al., 2005, 2011; Kreibich and Thieken, 2009; Poussin et al., 2012; Thurston et al., 2008). In Jakarta, measures are already taken at the household level, such as the building of second stories on houses so that valuable possessions can be moved upwards away from flood waters in the event of a flood, and using traditional building methods such as *rumah panggung* (elevated wooden house that stands on piles) in ways that are more commensurate with flooding (e.g. Marfai et al., 2015; Wijayanti et al., 2015). It would be of interest to assess the risk that could be achieved throughout the city if such measures were to be implemented on a larger scale, for example through the use of building codes. However, it should be noted that achieving all of the developments named above, including the situation depicted by the land use plan 2030 would entail very strong governance structures, strong spatial planning laws, and thorough implementation.

4454

5 Concluding remarks and future research developments

In this paper, we have extended the river flood risk model for Jakarta, developed by Budiyo et al. (2014), to include projections of flood risk under future scenarios of land subsidence, climate change (sea-level rise and changes in extreme precipitation), and land use change. Combining all of these scenarios, we find a median increase in flood risk of 263% in 2030 compared to baseline. This value is based on our median projection for the influence of changes in extreme precipitation on flood risk. However, since we found the influence of climate change on extreme precipitation to be highly uncertain, we also developed probabilistic projections of flood risk by developing PDFs based on 20 GCM-RCP combinations. The resulting increases in risk for the 5th and 95th percentiles are 189 and 336% respectively (when combined with the other drivers). This shows that whilst the influence of climate change on precipitation intensity in the region may be uncertain, when combined with the other drivers of risk, the increase is always large, and hence adaptation is imperative irrespective of the chosen climate scenario or projection.

The single driver with the largest influence on future flood risk is land subsidence (+173%). Clearly, addressing this driver could potentially have a large influence on reducing future flood risk. Land use change (+15%) and sea-level rise (+13%) lead to an increase in risk of the same order of magnitude as each other. We show that the largest share of total damages are found in land use classes related to commercial areas; these account for ca. 72% of total damages under current land use and 77% under future land use. However, in terms of area affected by flooding, residential areas have a great share. Hence, future efforts to reduce risk must focus on optimal land use planning for both classes (Aerts et al., 2005).

Whilst we have only examined river flood risk, Jakarta also experiences regular flooding due to coastal and flash flooding. The former has been assessed for Jakarta in Ward et al. (2011b), and Muis et al. (2015) have assessed both river and coastal flood risk at the scale of Indonesia using globally available datasets and models.

4455

Nevertheless, the impacts of river and coastal flooding can interact with each other – for example when high tides occur at the same time as extreme discharges – and this interaction should be a priority for future flood risk research, not just in Jakarta, but elsewhere (see, for example, Keef et al., 2009; Klerk et al., 2015; Svensson and Jones, 2001). To enable an assessment of these interactions, one would need to develop time-series of both high river discharge and high sea-levels, in order to examine the temporal interactions and joint probabilities between these two variables. However, at present long time-series of simulated sea levels are only available for limited regions (e.g. Haigh et al., 2013), although global modelling efforts may open this opportunity in the future.

Given the uncertainty in climate change projections, future development of official tailored climate scenarios for Jakarta (or indeed Indonesia) should be a research priority. Such a set of scenarios would allow for a more consistent modelling of climate impacts, not only in terms of flood risk analysis, but indeed in terms of climate impacts across a full range of hazards and sectors (e.g. Aerts et al., 2014).

Whilst we have simulated changes in hazard and exposure in the future, we have assumed that vulnerability remains constant over time. Recently, Jongman et al. (2015) showed that vulnerability to flooding has been reducing over the last 20–30 years in many developing countries. Hence, it would be useful to try to develop scenarios of potential vulnerability change in the future, and assess how this may affect the overall risk. Moreover, in the future projections we do not include adaptation measures that could be taken to reduce future risk (other than those measures that are already in place). Research by Muis et al. (2015) at the national scale for Indonesia has shown that the growth in future river and coastal flood risk could be contained to a large degree by increasing protection levels through the building of structural measures such as dikes, and by spatial zoning to limit developments in the most flood-prone locations, or at least to make future developments in those zones more commensurate with flooding. In our future work, we will use the model developed here to assess how the future increase in risk could potentially be decreased by: (1) the development of early warning

4456

- Works, Directorate General of Water Resources, Directorate of Rivers and Coastals, Jakarta, 2012.
- DTR DKI: Peta tata guna lahan provinsi, DKI, Jakarta, 2007.
- Erkens, G., Bucx, T., Dam, R., De Lange, G., and Lambert, J.: Sinking Coastal Cities, vol. 16, p. 14606, available at: <http://adsabs.harvard.edu/abs/2014EGUGA..1614606E>, last access: 22 April 2015, 2014.
- Guilyardi, E., Wittenberg, A., Fedorov, A., Collins, M., Wang, C., Capotondi, A., van Oldenborgh, G. J., and Stockdale, T.: Understanding El Niño in ocean–atmosphere general circulation models: progress and challenges, *B. Am. Meteorol. Soc.*, 90, 325–340, doi:10.1175/2008BAMS2387.1, 2009.
- Haight, I. D., Wijeratne, E. M. S., MacPherson, L. R., Pattiaratchi, C. B., Mason, M. S., Crompton, R. P., and George, S.: Estimating present day extreme water level exceedance probabilities around the coastline of Australia: tides, extra-tropical storm surges and mean sea level, *Clim. Dynam.*, 42, 121–138, doi:10.1007/s00382-012-1652-1, 2013.
- Hallegatte, S., Green, C., Nicholls, R. J., and Corfee-Morlot, J.: Future flood losses in major coastal cities, *Nature Climate Change*, 3, 802–806, doi:10.1038/nclimate1979, 2013.
- Hanson, S., Nicholls, R., Ranger, N., Hallegatte, S., Corfee-Morlot, J., Herweijer, C., and Chateau, J.: A global ranking of port cities with high exposure to climate extremes, *Climatic Change*, 104, 89–111, doi:10.1007/s10584-010-9977-4, 2010.
- Hempel, S., Frieler, K., Warszawski, L., Schewe, J., and Piontek, F.: A trend-preserving bias correction – the ISI-MIP approach, *Earth Syst. Dynam.*, 4, 219–236, doi:10.5194/esd-4-219-2013, 2013.
- Hendon, H. H.: Indonesian rainfall variability: impacts of ENSO and local air–sea interaction, *J. Climate*, 16, 1775–1790, doi:10.1175/1520-0442(2003)016<1775:IRVIOE>2.0.CO;2, 2003.
- Hulme, M. and Sheard, N.: *Climate Change Scenarios for Indonesia*, Climatic Research Unit, Norwich, UK, 1999.
- IPCC: Summary for policymakers, in: *Climate Change 2007: the Physical Science Basis*, contribution of Working Group I to the Fourth Assessment Report of the Intergovernmental Panel on Climate Change, edited by: Solomon, S., Qin, D., Manning, M., Chen, Z., Marquis, M., Averyt, K. B., Tignor, M., and Miller, H. L., Cambridge University Press, Cambridge, UK and New York, NY, USA, p. 13, 2007.
- IPCC: Summary for policymakers, in: *Climate Change 2014: Mitigation of Climate Change*, contribution of Working Group III to the Fifth Assessment Report of the Intergovernmental

4459

- Panel on Climate Change, edited by: Edenhofer, O., Pichs-Madruga, R., Sokona, Y., Farahani, E., Kadner, S., Seyboth, K., Adler, A., Baum, I., Brunner, S., Eickemeier, P., Kriemann, B., Savolainen, J., Schlömer, S., von Stechow, C., Zwicker, T., and Minx, J. C., Cambridge University Press, Cambridge, UK and New York, NY, USA, p. 21, 2014.
- JCDS: Jakarta Coastal Defence Strategy: Agenda, JCDS, Jakarta, Indonesia, 2011.
- Jeuken, A., Haasnoot, M., Reeder, T., and Ward, P. J.: Lessons learnt from adaptation planning in four deltas and coastal cities, *Journal of Water and Climate Change*, doi:10.2166/wcc.2014.141, online first, 2014.
- Jha, A., Bloch, R., and Lamond, J.: *Cities and Flooding: a Guide to Integrated Flood Risk Management for the 21st Century*, World Bank, Washington, DC, 2012.
- Jongman, B., Ward, P. J., and Aerts, J. C. J. H.: Global exposure to river and coastal flooding: long term trends and changes, *Global Environ. Chang.*, 22, 823–835, doi:10.1016/j.gloenvcha.2012.07.004, 2012.
- Jongman, B., Winsemius, H. C., Aerts, J. C. J. H., de Perez, E. C., van Aalst, M. K., Kron, W., and Ward, P. J.: Declining vulnerability to river floods and the global benefits of adaptation, *P. Natl. Acad. Sci. USA*, 112, E2271–E2280, doi:10.1073/pnas.1414439112, 2015.
- Keef, C., Svensson, C., and Tawn, J. A.: Spatial dependence in extreme river flows and precipitation for Great Britain, *J. Hydrol.*, 378, 240–252, doi:10.1016/j.jhydrol.2009.09.026, 2009.
- Kementerian Koordinator Bidang Perekonomian: Draft Master Plan Pengembangan Terpadu Pesisir Ibukota Negara (PTPIN), Jakarta, 1 April 2014.
- Klerk, W. J., Winsemius, H. C., van Verseveld, W. J., Bakker, A. M. R., and Diermanse, F. L. M.: The co-occurrence of storm surges and extreme discharges within the Rhine? Meuse Delta, *Environ. Res. Lett.*, 10, 035005, doi:10.1088/1748-9326/10/3/035005, 2015.
- Kreibich, H. and Thielen, A. H.: Coping with floods in the city of Dresden, Germany, *Nat. Hazards*, 51, 423–436, 2009.
- Kreibich, H., Thielen, A. H., Petrow, Th., Müller, M., and Merz, B.: Flood loss reduction of private households due to building precautionary measures – lessons learned from the Elbe flood in August 2002, *Nat. Hazards Earth Syst. Sci.*, 5, 117–126, doi:10.5194/nhess-5-117-2005, 2005.
- Kreibich, H., Christenberger, S., and Schwarze, R.: Economic motivation of households to undertake private precautionary measures against floods, *Nat. Hazards Earth Syst. Sci.*, 11, 309–321, doi:10.5194/nhess-11-309-2011, 2011.

4460

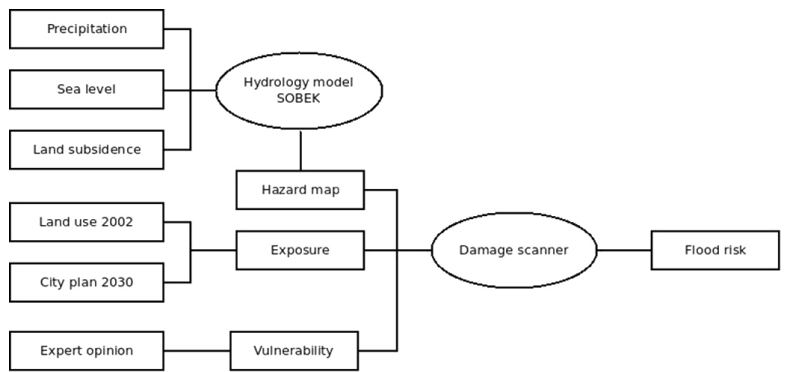


Figure 1. Framework of analysis.

4471

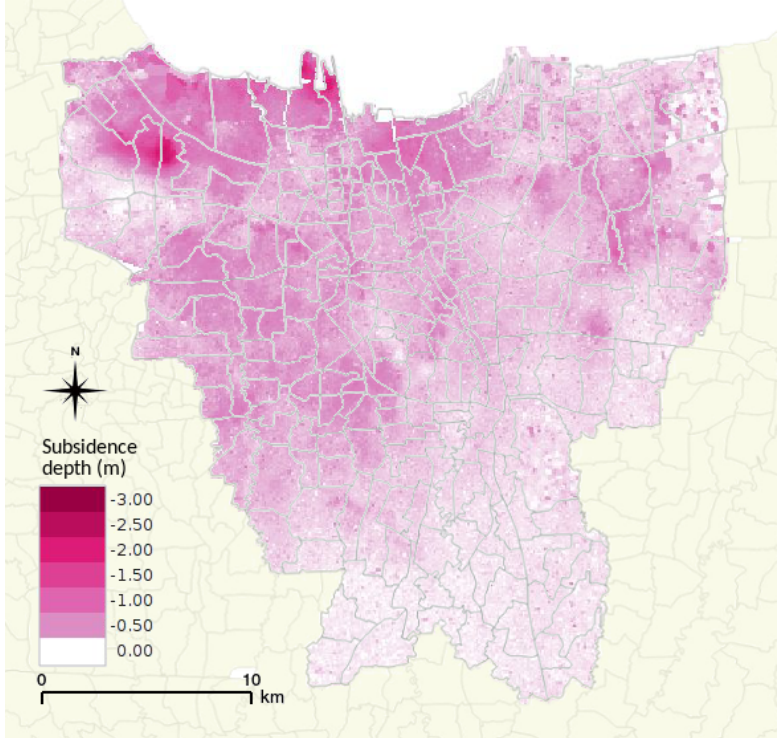


Figure 2. Spatial distribution of projected total land subsidence over the period 2012–2025.

4472

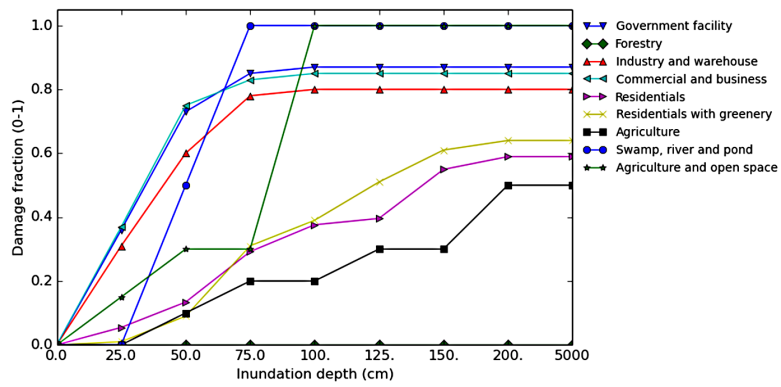


Figure 3. Vulnerability curves used in this study for each land use map plan 2030.

4473

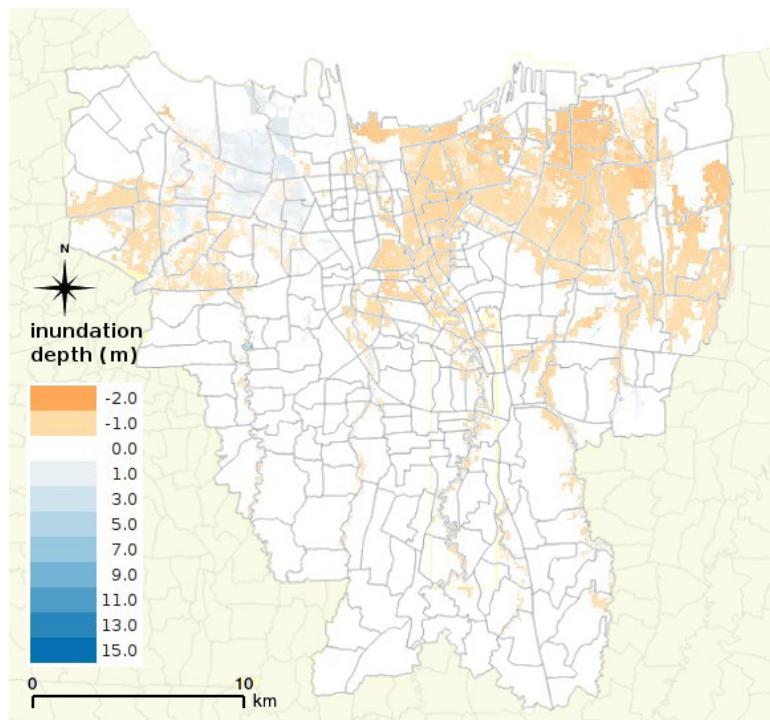


Figure 4. Change in inundation depth for a return period of 100 years in the flood hazard maps based on the SOBEK schematisation of 2013 compared to that of 2007.

4474

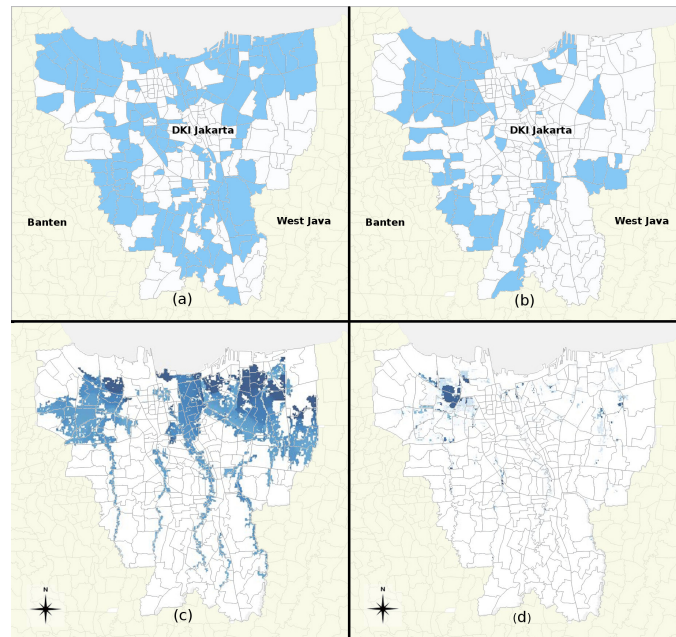


Figure 5. Maps showing Kelurahan (village administration units) in which part of the village administration unit was reported to be inundated in the (a) 2007 and (b) 2013 floods. These maps are reported to the National Disaster Management Office (BNPB) by the village administrator. The estimated return periods of the flood events in 2007 and 2013 are 50 and 30 respectively. Underneath, the inundation maps from the SOBEK model are shown based on: (c) 2007 schematisation and a return period of 50 years; and (d) 2013 schematisation and a return period of 25 years.

4475

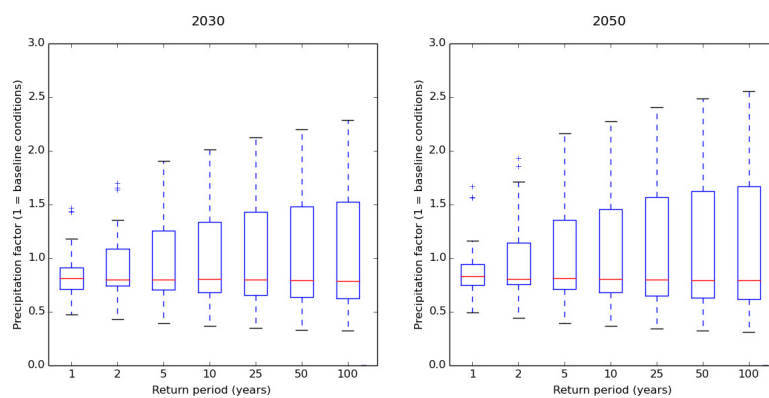


Figure 6. Box and whisker plots showing the distributions of precipitation factors (where a factor of “1” equals baseline conditions) for extreme 1 day precipitation for several return periods, ranging from 1 to 100 years. The results are shown for 2030 and 2050. The results are based on 5 GCMs and 4 RCPs. The boxplots show the median values for the 20 GCM-RCP combinations (red lines); the 25th and 75th percentiles (top and bottom of boxes); and the range (whiskers). Outliers as shown as “+”.

4476

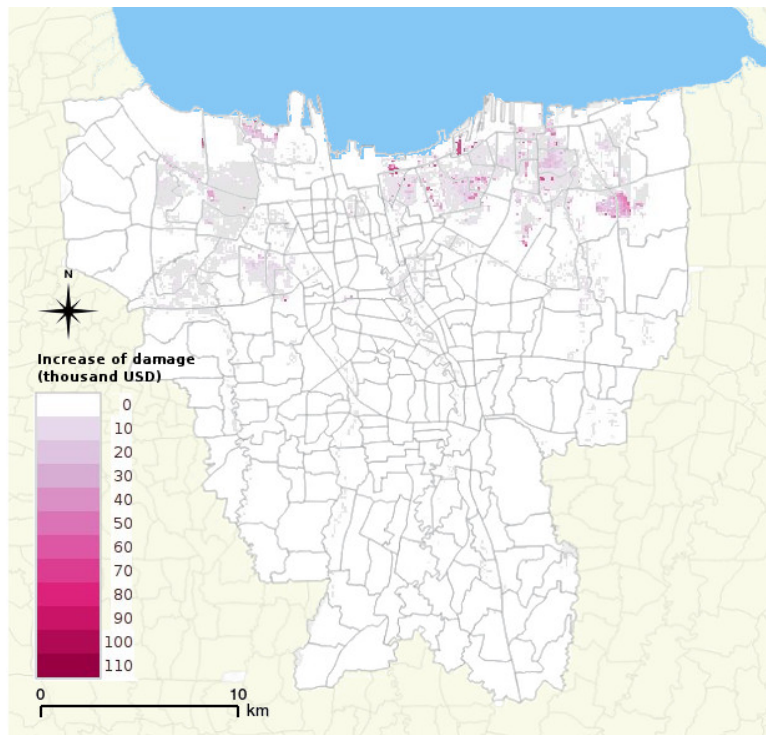


Figure 7. Increase of damage per grid cell at return period 100 between current and 2007 map due to land subsidence alone.

4477

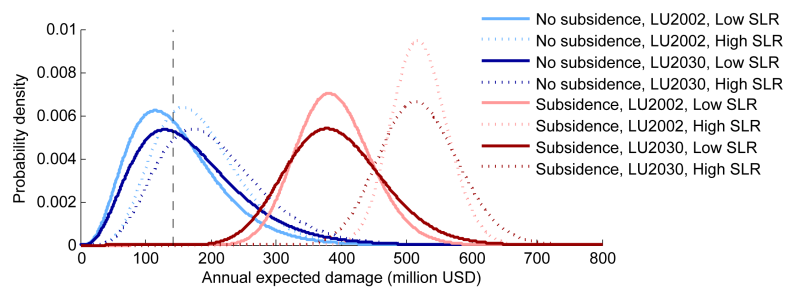


Figure 8. Probability distribution function (PDFs) of future flood risk in Jakarta under different scenarios. The black vertical dashed line shows risk associated with current conditions (USD 143 million p.a.). The PDFs are obtained by applying a two-parameter gamma distribution to simulated risk values from 5 GCMs and 4 RCP emission scenarios. PDFs are shown for different combinations of the following scenarios: **(a)** subsidence and no subsidence; **(b)** land use under baseline conditions (LU2002) and under the land use plan for 2030 (LU2030); and **(c)** high or low sea level rise (SLR).

4478